Proceedings World Geothermal Congress 2020+1
Reykjavik, Iceland, April - October 2021

Evaluation of Silica Scale Inhibitors

Michael A. Todd

Solenis LLC, 500 Hercules Rd., Wilmington, DE, 19808

mtodd@solenis.com

Keywords: silica, scale, inhibition, amorphous, aluminum, polymerization

ABSTRACT

Silica scale is a serious problem for many geothermal power plants. Deposition of amorphous silica can occur when the temperature drops, causing the silica solubility to decrease. Once formed, silica scale restricts the water flow and reduces the efficiency of heat exchangers and the reinjection capacity of reinjection wells. Further complicating things, silica can precipitate as either amorphous silica or as a metal silicate, such as magnesium silicate. Laboratory experiments to mitigate both types of scale have been initiated.

A variety of inhibitors were evaluated at pH 7.0 using the molybdate active silica test. The best inhibitors prevented the polymerization of silica at least four hours, even at low doses. Silica polymerization was prevented using as little as 10 ppm of inhibitor. Leading candidates were further tested in the presence of poisons such as aluminum. Several of the most effective inhibitors of amorphous silica polymerization were ineffective in the presence of aluminum silicate. This work describes the progress toward the development of scale inhibitors that prevent amorphous silica scale in the presence of aluminum.

1. INTRODUCTION

Silica is ubiquitous in geothermal water. Silica becomes soluble when silica-containing rock contacts hot geothermal water. As the temperature increases so does the solubility of silica (Zuhl and Amjad, 2014). Some silica dissolves in the hot reservoir water. Often, geothermal brine is at or near saturation limit it reaches the surface. When geothermal power plants extract heat from the brine, the temperature drops, leading to lower silica solubility. When the silica solubility drops below the silica concentration, silica scaling can occur. Often, scale forms in steam separators and heat exchangers, leading to restricted flow and reduced energy extraction. Scale negatively influences the amount of electricity that can be produced and reduces the return on investment from geothermal power plants. A need exists for a silica scale inhibitor that prevents silica polymerization and eliminates the formation of amorphous silica. Previous studies experienced mixed success with silica scale inhibitors (Gallup, 1993; Gallup, 1997; Gallup, 2002; Gallup and Barcelon, 2005; Garcia et al., 2001). While some efficacy was observed in the laboratory and in the field, most inhibitors did not completely inhibit amorphous silica scale. In fact, several inhibitors *caused* increased deposition in laboratory and field tests (Gallup, 2002; Gallup and Barcelon, 2005). Increased deposition has been observed even under non-geothermal conditions (Demadis and Neofotistou, 2007; Demadis et al., 2009; Mavredaki et al., 2005; Zhang et al., 2011; Zhang et al., 2012A; Zhang et al., 2012B). This study was initiated to develop an amorphous silica scale inhibitor which prevents silica polymerization without causing precipitation or flocculation of silica colloids.

Silica scaling is complicated and involves a number of different steps which have been discussed fully elsewhere (Bergna and Roberts, 2006). Briefly, polymerization of silicic acid, formation of silica colloids, colloid growth, precipitation and flocculation all are involved. Each of the steps is affected differently by temperature, pH and water chemistry. Together, the steps lead to a complex process in which silica can scale through four different mechanisms.

1. Silica Polymerization, Amorphous Silica Colloid Formation and Growth

2. Charge neutralization/agglomeration of amorphous silica colloids

3. Initiation of silica polymerization by metal silicates or hydroxides

4. Metal silicate formation

1.1 Silica Polymerization, Amorphous Silica Colloid Formation and Growth

The first mechanism of silica scale formation involves the polymerization of silica followed by colloid formation. Silicic acid initially dimerizes and then polymerizes to form polysilicic acid. Additional polymerization eventually leads to the formation of amorphous silica colloids. Temperature, pH, conductivity and a variety of anions and cations affect both the polymerization process and colloid formation (Weres et al., 1981; Amjad and Zuhl, 2010; Ngothai et al., 2012). These colloids continue to grow by reacting with silicic acid in solution, as shown in Figure 1, as long as the concentration of silicic acid in solution exceeds the silica saturation limit. Commonly referred to as amorphous silica because they do not have a well-defined crystalline structure, these colloids are slightly negatively charged and, when small, are readily dispersed in water. This dispersion is the result of both electrostatic repulsion from the negative charge and steric repulsion from polysilicate chains on the surface of the colloid (Chen et al., 2018). As the colloids grow in size, however, these forces are no longer strong enough to keep the particles dispersed, leading to deposition (Bergna and Roberts, 2006). Given enough time, silica will polymerize until it reaches the silica saturation limit. This mechanism requires the silica concentration to be greater than the silica saturation limit.

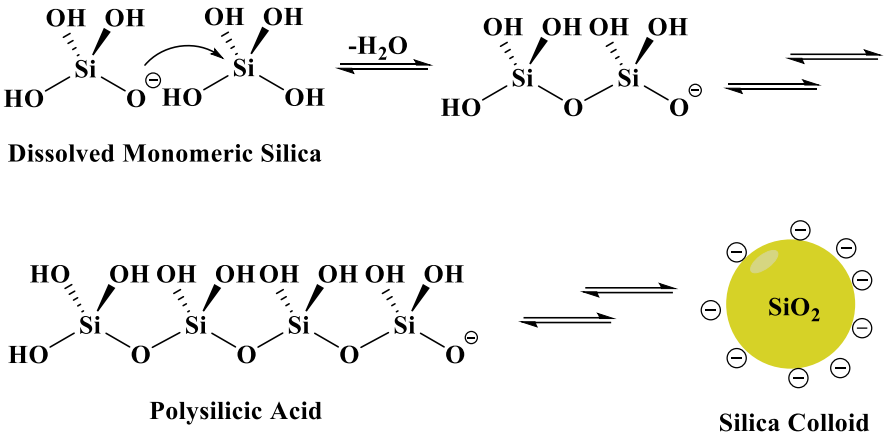

Figure 1. Polymerization of silica to polysilicic acid and eventual formation of colloidal silica.

1.2 Charge Neutralization/Agglomeration of Amorphous Silica Colloids

Another mechanism of deposition is charge neutralization and agglomeration. Negatively charged silica colloids can be neutralized by positively charged cations such as Ca^{2+}, Mg^{2+}, Al^{3+}, $Fe^{2+/3+}$. Neutralization of the negative charge reduces the electrostatic repulsion between the colloids, thereby reducing the dispersibility of the colloids and leading to fine particles and possibly floc, which can deposit on surfaces (Iler, 1975; Nishida et al., 2009). In this mechanism, silica precipitates and flocculates more readily than amorphous silica alone. This mechanism requires the silica concentration to be greater than the saturation limit and high levels of di or trivalent cations to be available to neutralize the silica colloids.

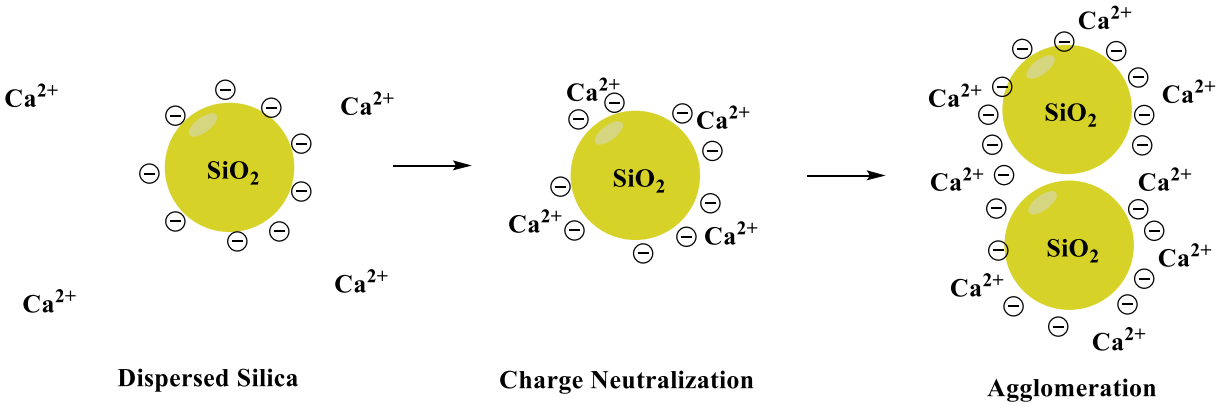

Figure 2. Charge neutralization and agglomeration of colloidal silica.

1.3 Initiation of Silica Polymerization by Metal Silicates or Hydroxides

Silica polymerization can also be initiated by metal hydroxides or metal silicates. In this mechanism, a metal oxide, ($M\text{-}O^-$) or silicate ($Si\text{-}O^-$) functional group can initiate polymerization, thereby causing the growth of amorphous silica on either colloids suspended in solution or on surface deposits. Eventually, enough silica deposits such that the scale becomes mostly amorphous silica. Although, the polymerization and colloid formation steps are identical to those of amorphous silica, the initiation step is different. Silica can polymerize below the silica saturation limit if polymerization is initiated by a metal silicate (Newton et al., 2018; Johnston et al., 2018). This mechanism requires the presence of a metal hydroxide or a metal silicate. Therefore, the concentration of the initiator (metal hydroxide or metal silicate) must exceed the solubility limit, which is influenced heavily by the pH and the metal concentration levels. The formation of iron, magnesium, calcium or aluminum silicates must be avoided to control this type of scale.

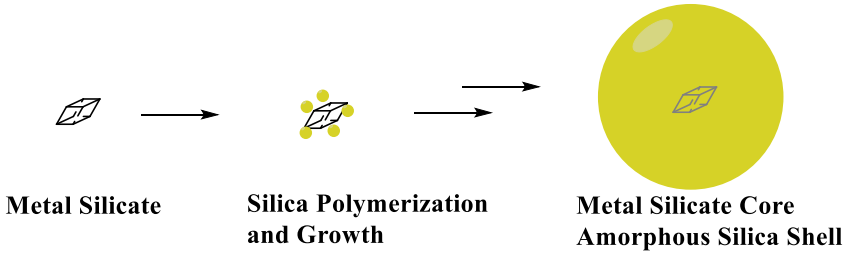

Figure 3. Silica growth on a metal silicate crystal.

1.4 Metal Silicate Formation

The final mechanism is the formation of crystalline metal silicate. This mechanism does not involve amorphous silica or silica polymerization and has a well-defined crystalline structure. Metal silicates often have very different saturation levels than silica and are influenced heavily by the concentration of the metal cation, temperature and pH. Silicates of iron, magnesium and aluminum are common in geothermal systems (Inali and Atilla, 2011; Newton et al., 2018). These scales typically are controlled using either a dispersant or a crystal modifier (Gonzalez et al., 2003). The control of metal silicates is beyond the scope of this work, which focuses on the control of amorphous silica scale.

2. EXPERIMENTAL SECTION

The silica stock solution was prepared by dissolving 5.68 g of sodium metasilicate nonahydrate in 94.32 g of deionized water. This solution was used within 1 hour of preparation and was remade daily. A stock solution of calcium/magnesium was prepared by dissolving 29.4 g of calcium chloride dihydrate and 40.7 g of magnesium chloride hexahydrate in 929.9 g of deionized water. Inhibitors were dissolved in water to make a 1% inhibitor solution by weight. Aluminum chloride hexahydrate was also dissolved in solution to make a 0.1 % Al^{3+} solution by weight.

2.1 Polymerization Inhibition Tests

Ninety-two and one half grams of water were added to a 125 mL polyethylene bottle. One half gram of 20% hydrochloric acid was added. This solution was placed on a shaker table, shaken at 200 rpm and heated to the desired temperature. After 45 minutes, the solution was removed. Four and three tenths mL of the silica stock solution was added, followed by 0.1 mL of the inhibitor stock solution and 2.5 mL of the calcium/magnesium stock solution. Optionally, 0.1 mL of a solution of 0.1% aluminum chloride as aluminum was added. The pH of this solution was approximately 3 and was adjusted to 7.0 +/- 0.1 using sodium hydroxide. When the pH was raised to 7.0 the time was recorded as t = 0 minutes.

Silica polymerization was analyzed using a Hach™ DR3900 using the HR Silica test method. A 1 mL aliquot was added to 9 mL of deionized water in a 1-inch square sample cell from Hach. To this solution was added sodium molybdate followed by sulfamic acid. After 10 minutes, citric acid was added. After an additional 2 minutes, the concentration of silica was measured at 452 nm and was expressed as ppm as SiO_2. Readings were taken periodically to establish a time course for the polymerization of silica.

Table 1. Water Chemistry for Silica Polymerization Tests at 40 ˚C.

Silica as SiO_2	550 ppm
Ca^{2+}	200 ppm
Mg^{2+}	122 ppm
pH	7.0
Temperature	40 ^{o}C
Silica Saturation Index	3.6

2.2 Turbidity Measurements

Turbidity was measured using a Hach™ 2100Q turbidimeter. Approximately 10 mL of sample was poured into a sample cell and measured immediately. Results are expressed as nephelometric turbidity units, NTU. Turbidity measurements were taken at the same time as silica polymerization measurements. An increase in turbidity indicated an increase in precipitation and/or flocculation.

3. RESULTS AND DISCUSSION

The concentration of silica was measured over time in order to investigate the efficacy of the silica polymerization inhibitors. The starting silica concentration was 550 ppm as SiO_2. Successful inhibitors maintained a high silica reading throughout the experiment, while unsuccessful inhibitors allowed the silica level to drop over the course of the experiment.

3.1 Polymerization Inhibition

Polymers and small molecules were screened for polymerization inhibition at 40 ˚C for 4 hours, as shown in Figure 4. These tests were run in the absence of aluminum. In the absence of inhibitor, the concentration of reactive silica dropped from more than 500 ppm to approximately 300 ppm as SiO_2. Several inhibitors failed to inhibit polymerization and the decline in silica concentration was comparable to the control experiment. Inhibitor I9 appeared to increase the rate of silica polymerization. Four inhibitors successfully kept the reactive silica concentration above 500 ppm for the duration of the experiment. The most successful polymers were a nonionic polymer, I7; an amine based polymer, I8; and two carboxylated polymers, I5 and I6.

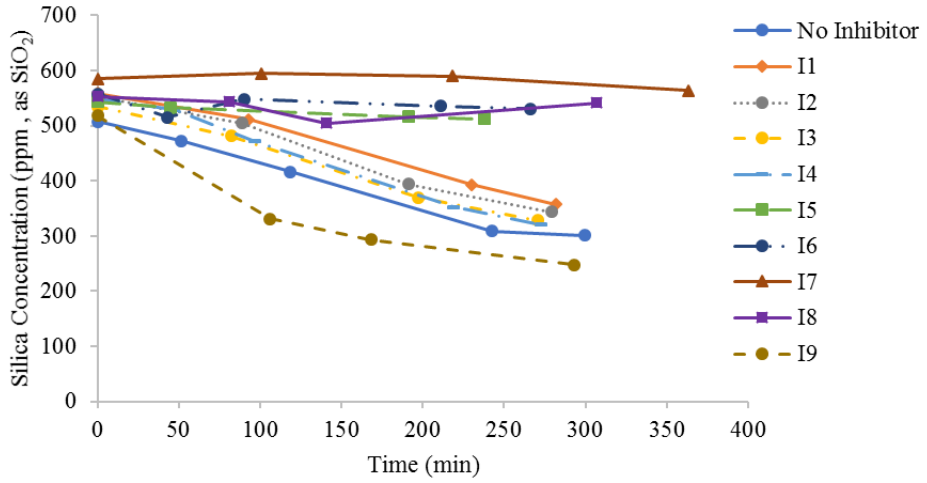

Figure 4. Silica inhibition by 10 ppm of inhibitor. Temperature = 40 °C, pH = 7.0, 550 ppm silica as SiO_2, 122 ppm Mg^{2+}, 200 ppm Ca^{2+}. Silica saturation index, SSI = 3.6.

The effect of pH on the efficacy of Inhibitor I7 was investigated. This inhibitor was dosed at 10 ppm at pH equals 7.0, 7.5, 8.0 and 8.5. At pH less than or equal to 7.5, this inhibitor inhibits silica polymerization, as shown in Figure 5. When pH is raised to 8.0 or 8.5, Inhibitor I7 loses efficacy and silica rapidly polymerizes. Most likely this is due to the formation of magnesium silicate. Throughout these tests, when pH equals 7.5, the magnesium silicate saturation index is less than 1; however, when pH equals 8.0, the index rises to 5.5, as shown in Table 2. Based on these results, I7 works well at preventing amorphous silica formation but does not prevent magnesium silicate formation. Other products have been developed that do prevent the formation of calcium and magnesium silicate scale through dispersion (Gonzalez et al., 2003; Garcia and Mejorada, 2001).

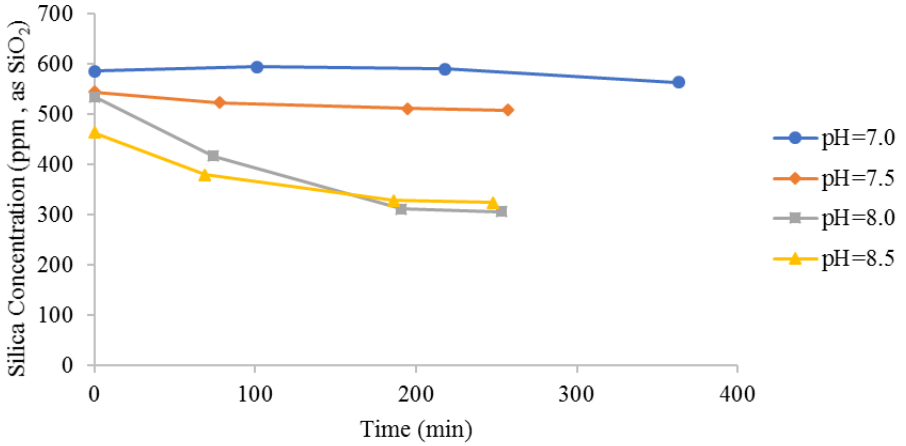

Figure 5. Effect of pH on the efficacy of 10 ppm of I7. Temperature = 40 °C, pH = 7.0, 550 ppm silica as SiO_2, 122 ppm Mg^{2+}, 200 ppm Ca^{2+}. Silica saturation index, SSI = 3.6.

Table 2. Effect of pH on the Magnesium and Silica Saturation Indexes.

Temperature	40 °C	40 °C	40 °C	40 °C
pH	7.0	7.5	8.0	8.5
Silica Concentration (ppm, as SiO_2)	550	550	550	550
Magnesium Concentration (ppm)	122	122	122	122
Silica Saturation Index	3.6	3.6	3.5	3.3
Magnesium Silicate Saturation Index	0.1	0.6	5.5	50.2

3.2 Effect of Aluminum

Next, Inhibitors I5–I8 were tested in the presence of aluminum. Reactions were run using 550 ppm of silica, as SiO_2; 1 ppm of Al^{3+}; pH equals 7.0; and temperature equals 40 °C. Under these aggressive conditions, the inhibitors failed to prevent polymerization of silica, as shown in Figure 6. The presence of 1 ppm of aluminum reduced the efficacy of these inhibitors to the point that they were able to reduce only slightly the rate of silica polymerization. Over the course of 4 to 5 hours, more than 200 ppm of silica was polymerized. Each of these inhibitors, I5–I8, prevented silica polymerization in the absence of aluminum, as shown in Figure 1, but

failed to prevent silica polymerization in the presence of 1 ppm of aluminum, as shown in Figure 6. Two possible explanations exist for this behavior.

1. Inhibitors could be poisoned by Al^{3+}, thereby reducing their efficacy. This effect has been noted before (Amjad and Zuhl, 2009). In this mechanism, aluminum interacts with the inhibitor and prevents it from interacting with the silica. The inhibitor thus becomes deactivated and efficacy is reduced.

2. Aluminum could be catalyzing or initiating silica polymerization. Aluminum can cause silica polymerization below the silica saturation limit (Newton et al., 2018). This is the mechanism shown in Figure 3, where a metal silicate initiates silica polymerization. Polymers I5–I8 may be effective in preventing amorphous silica polymerization but ineffective at preventing polymerization caused by metal silicates.

It is unclear which of these mechanisms is operative under these conditions. Regardless, this is a serious issue because aluminum is present in many geothermal brines and is incorporated into many silica containing scales. Successful inhibitors must tolerate and mitigate the effects of aluminum.

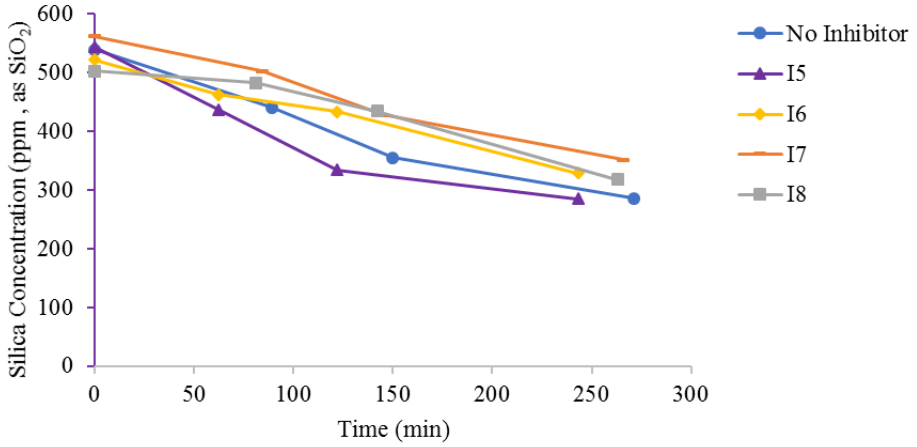

Figure 6. Effect of aluminum on the efficacy of silica polymerization Inhibitors I5–I8. Temperature = 40 ˚C, pH = 7.0, 550 ppm silica as SiO_2, 122 ppm Mg^{2+}, 200 ppm Ca^{2+}, 1 ppm Al^{3+}. Silica saturation index, SSI = 3.6.

Inhibitors I7 and I8 were tested in combination with other inhibitors to investigate any synergistic combinations. Inhibitor I7 was dosed at 10 ppm with 10 ppm of other inhibitors, as shown in Figure 7. In all cases, these combinations failed to prevent silica polymerization. The best results were obtained with the combination of I7 and inhibitor I11 or I8 or I14 or I19 in which silica polymerization was slowed, but was not completely arrested. The combination of I7 and I11 was superior to the other combinations; however, even it still allowed approximately 100 ppm of silica to be polymerized over the course of the experiment. Inhibitors I5, I6, I9, I13, I15, I18 and I20 did not have a significant effect on the observed polymerization rate.

Inhibitor I8 was then tested in combination with other inhibitors. None of the combinations completely inhibited silica polymerization, as shown in Figure 8. The most effective combination was with Inhibitors I8 and I11, which reduced the amount of polymerized silica by approximately 150 ppm over a 4 hour time period. Interestingly, at 10 ppm, I11 alone did not inhibit silica polymerization, as shown in Figure 8 and was no different from the control without inhibitor. Inhibitor I11 appears to work synergistically with Inhibitors I7 and I8 to provide additional polymerization inhibition. Under these conditions, silica polymerization was not completely inhibited but was reduced by approximately 150 ppm over the 4 hour experiment relative to the control without added inhibitor.

3.3 Turbidity Measurements

While these inhibitors were successful in slowing the observed silica polymerization rate, some precipitation and flocculation was observed in all tests, including the most successful tests using the combinations of I7 and I11 and I8 and I11. This is quantified as shown in Figures 9-11. Over time, the inhibitors prevented polymerization; however, increasing amounts of precipitation was observed and was quantified as increased turbidity. This trade off was observed for all inhibitors that prevented polymerization. Gallup previously observed this effect for inhibitors in geothermal applications. When Geogard™ SX was applied at low doses, scale formation was partially prevented. At higher doses, scale formation *increased*, suggesting that Geogard™ SX disrupted silica dispersion at higher doses (Gallup, 2002; Gallup and Barcelon, 2005). Other authors have observed similar effects during experimental studies (Demadis and Neofotistou, 2007; Demadis et al., 2009; Mavredaki et al., 2005; Zhang et al., 2011; Zhang et al., 2012A; Zhang et al., 2012B). These inhibitors likely do not prevent polymerization entirely and thus colloids do form. The inhibitors subsequently *cause flocculation* of the colloids, thereby leading to turbidity.

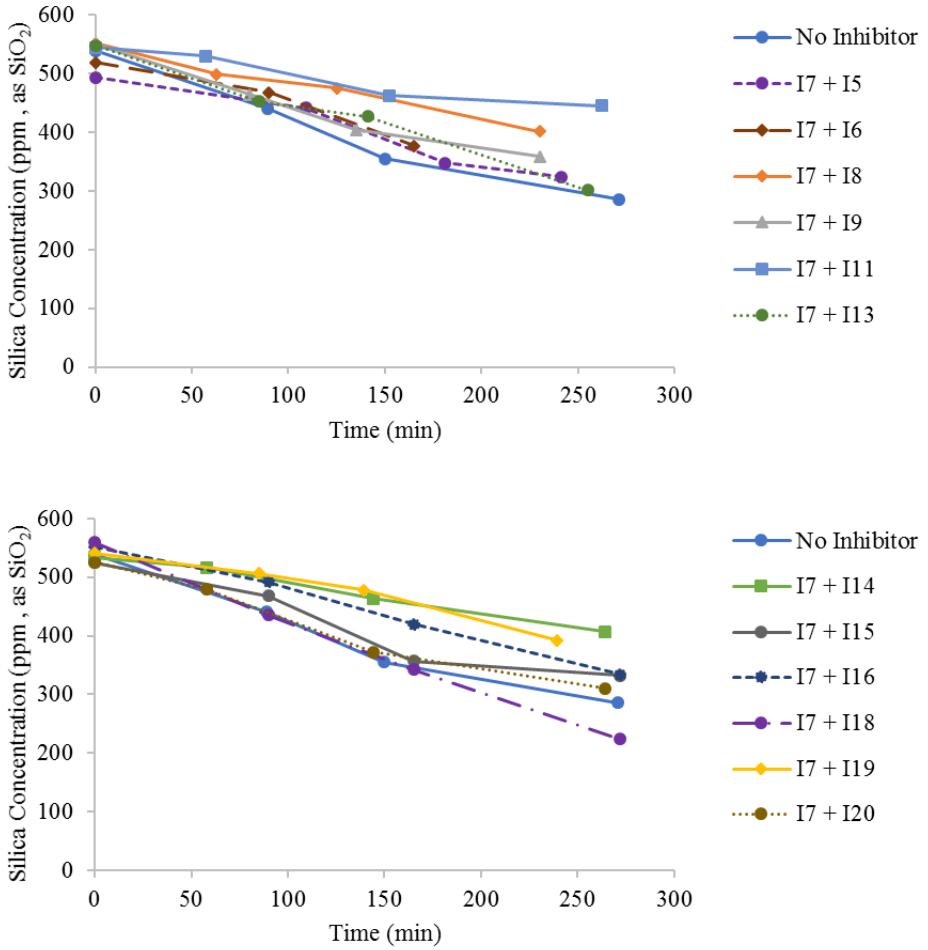

Figure 7. Efficacy of combinations of Inhibitor I7 with other inhibitors. All inhibitors were dosed at 10 ppm. Temperature = 40 ˚C, pH = 7.0, 550 ppm silica as SiO_2, 122 ppm Mg^{2+}, 200 ppm Ca^{2+}, 1 ppm Al^{3+}. Silica saturation index, SSI = 3.6.

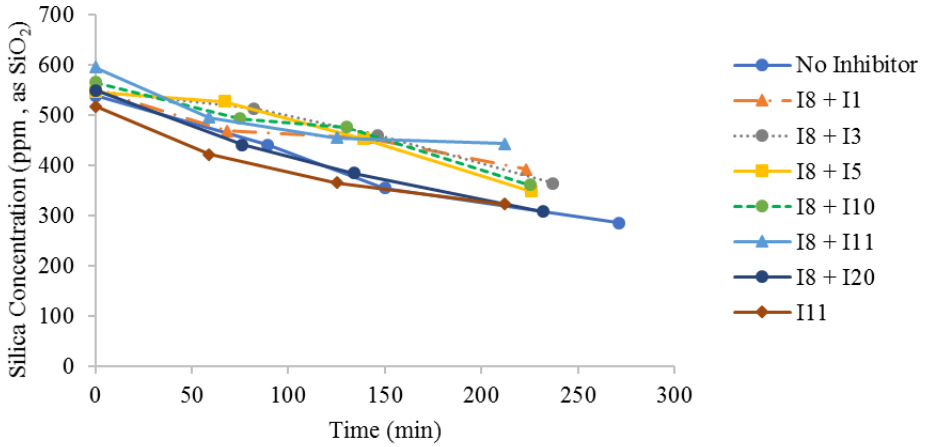

Figure 8. Efficacy of combinations of Inhibitor I8 with other inhibitors. All inhibitors were dosed at 10 ppm. Temperature = 40 ˚C, pH = 7.0, 550 ppm silica as SiO_2, 122 ppm Mg^{2+}, 200 ppm Ca^{2+}, 1 ppm Al^{3+}. Silica saturation index, SSI = 3.6.

A dose response was run using Inhibitors I8 and I11, as shown in Figure 9. The concentration of I11 was held constant at 10 ppm while the concentration of I8 was varied from 0 to 10 ppm. Both the silica concentration and turbidity were measured over time. Using 0 ppm of I8 and 10 ppm of I11, the silica polymerized but the turbidity stayed low. No signs of precipitation or flocculation were visible. Presumably, small silica polymers and colloids did form but remained small and well dispersed throughout the experiment. As the concentration of I8 was increased, the polymerization slowed but the turbidity increased. At 6 ppm of I8, the turbidity increased to 19 NTU and precipitation was visible. At 8 ppm and 10 ppm of I8, polymerization slowed even further, but the turbidity increased to 33 NTU. Precipitation and flocculation were both observed. These results suggest that while I8 can slow silica polymerization, it does not prevent it completely. Silica probably polymerizes to form polymers and small colloids. The inhibitor then *causes* the precipitation and flocculation of the colloids into visible precipitant and floc. Silica is known to disperse

well without added inhibitor (Bergna and Roberts, 2006). This dispersability is a combination of electrostatic repulsion and steric repulsion from polysilicate chains on the colloid surface (Chen et al., 2018). Inhibitors can disrupt either the electrostatic repulsion through charge neutralization or the steric repulsion by interacting with the polysilicate chains on the colloid surface. Cationic inhibitors disrupt the dispersability mainly through charge neutralization. Non-ionic and anionic inhibitors mainly affect dispersion by interacting with the polysilicate chains and disrupting the steric repulsion.

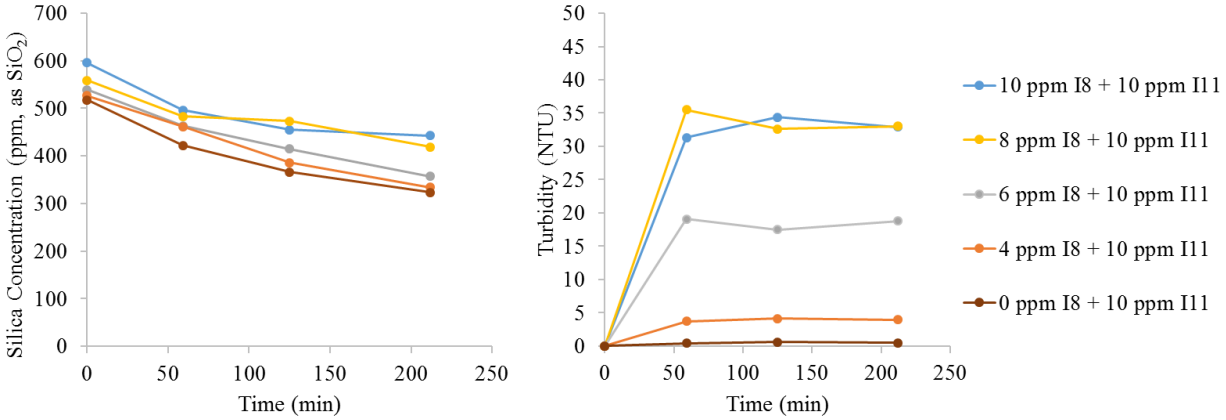

Figure 9. Efficacy of combinations of Inhibitor I8 with other inhibitors. All inhibitors were dosed at 10 ppm. Temperature = 40 ˚C, pH = 7.0, 550 ppm silica as SiO_2, 122 ppm Mg^{2+}, 200 ppm Ca^{2+}, 1 ppm Al^{3+}. Silica saturation index, SSI = 3.6. Left: Silica polymerization. Right: Turbidity.

3.4 Tests at 60 ˚C; SSI = 2.6

At a temperature of 40 ˚C, the silica saturation index, SSI, was 3.6, which was quite aggressive. Raising the temperature to 60 ˚C lowers the SSI to 2.6, which was considerably less aggressive. Some of the tests were repeated at 60 ˚C under otherwise identical conditions. The water chemistry is detailed in Table 3.

Table 3. Water Chemistry for Experiments at 60 °C.

Silica as SiO_2	550 ppm
Ca^{2+}	200 ppm
Mg^{2+}	122 ppm
Al^{3+}	1 ppm
pH	7.0
Temperature	60 ˚C
Silica Saturation Index	2.6

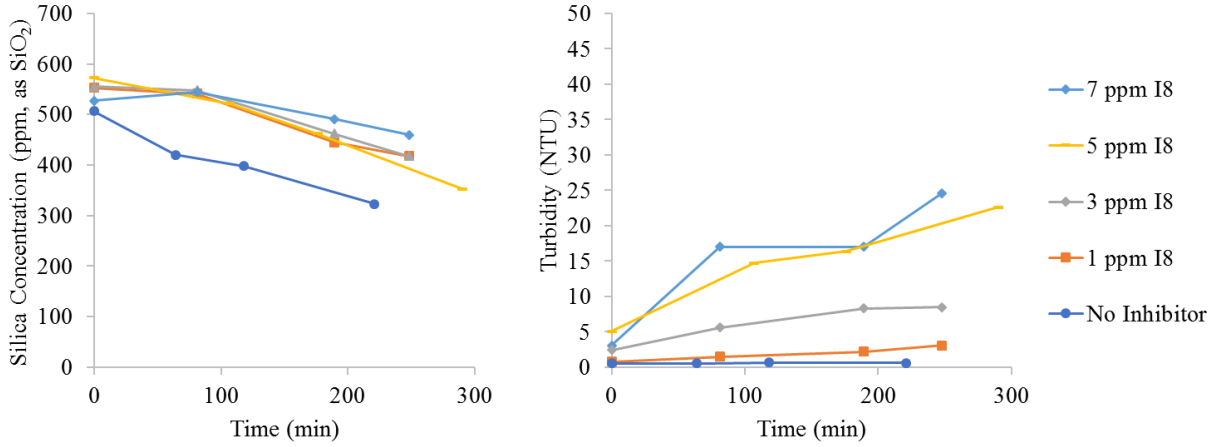

Figure 10. Dose response of I8. Temperature = 60 ˚C, pH = 7.0, 550 ppm silica as SiO_2, 122 ppm Mg^{2+}, 200 ppm Ca^{2+}, 1 ppm Al^{3+}. Silica saturation index, SSI = 2.6. Left: Silica polymerization inhibition. Right: Turbidity.

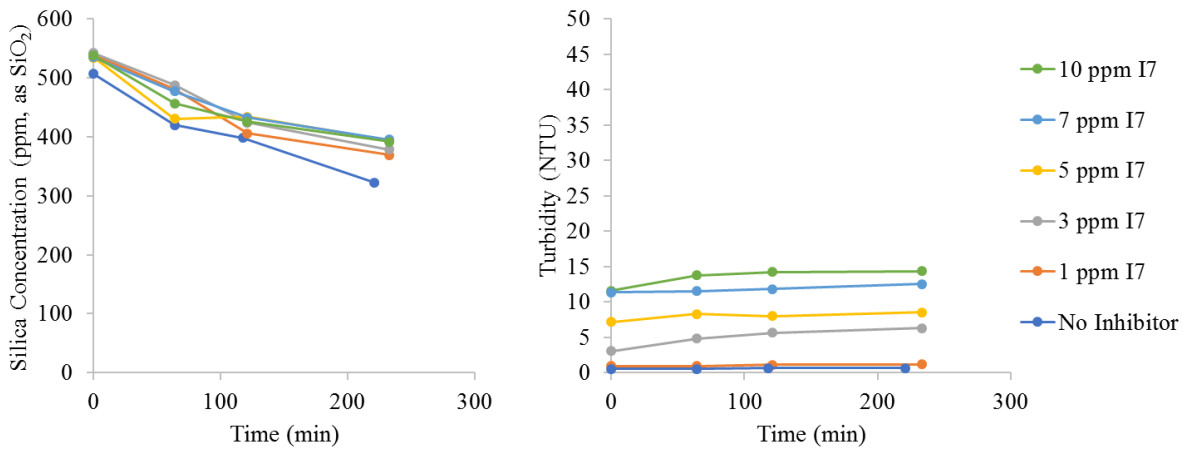

Figure 11. Dose response of I7. Temperature = 60 ˚C, pH = 7.0, 550 ppm silica as SiO_2, 122 ppm Mg^{2+}, 200 ppm Ca^{2+}, 1 ppm Al^{3+}. Silica saturation index, SSI = 2.6. Left: Silica polymerization inhibition. Right: Turbidity.

A dose response of Inhibitors I8 and I7 was run at a temperature of 60 ˚C, as shown in Figures 10 and 11. Both inhibitors slowed but did not prevent silica polymerization. As expected, an increase in the inhibitor dose led to a reduction in silica polymerization. Unfortunately, increased doses also significantly increased the turbidity of the solution. At 1 ppm, neither inhibitor produced a significant amount of turbidity. At 7 ppm, both inhibitors caused a significant amount of precipitation and flocculation, which was quantified as increased turbidity. This effect was not the same for both inhibitors. Inhibitor I8 caused significantly more turbidity than I7 (25 NTU with 7 ppm I8 vs. 14 NTU with 7 ppm I7.) This effect is consistent with previous work by Gallup, who showed increased precipitation with increased doses of inhibitors (Gallup, 2002; Gallup and Barcelon, 2005).

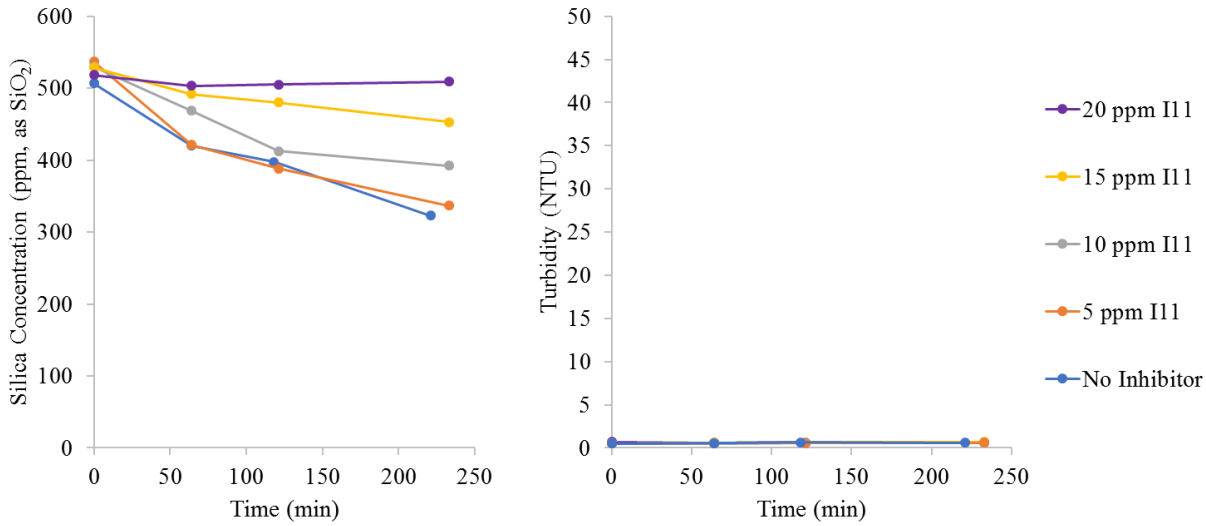

Figure 12. Dose response of I11. Temperature = 60 ˚C, pH = 7.0, 550 ppm silica as SiO_2, 122 ppm Mg^{2+}, 200 ppm Ca^{2+}, 1 ppm Al^{3+}. Silica saturation index, SSI = 2.6. Left: Silica polymerization inhibition. Right: Turbidity.

A dose response of Inhibitor I11 from 5 to 20 ppm was also investigated. At 5, 10 and 15 ppm, I11 reduced but failed to prevent silica polymerization. At 20 ppm, however, I11 prevented silica polymerization, as shown in Figure 12. The measured turbidity was less than 1 NTU for all doses. Inhibitor I11 was then tested in combination with I7, as shown in Figure 13. The concentration of I7 was kept constant at 5 ppm while the concentration of I11 was varied between 5 and 20 ppm. The combination of these inhibitors prevented silica polymerization and precipitation at all concentrations. Even the combination of 5 ppm of I7 and 5 ppm of I11 prevented polymerization for more than 2 hours. No turbidity was observed in any of the experiments with the combination of I7 and I11. These results were very different from those observed with each inhibitor individually. Neither I7 nor I11 provided complete protection at either 5 or 10 ppm. Furthermore, I7 caused precipitation at both 5 and 10 ppm. The combination of I7 and I11, however, led to reduced silica polymerization without increased precipitation. The exact mechanism of the inhibition by this combination is under investigation.

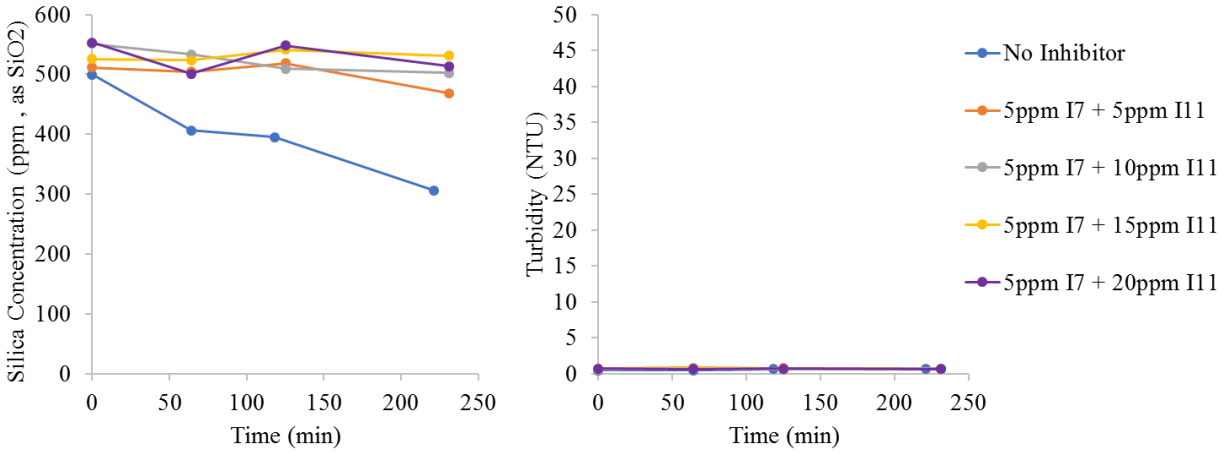

Figure 13. Synergy between I7 and I11. Temperature = 60 ˚C, pH = 7.0, 550 ppm silica as SiO_2, 122 ppm Mg^{2+}, 200 ppm Ca^{2+}, 1 ppm Al^{3+}. Silica saturation index, SSI = 2.6. Left: Silica polymerization inhibition. Right: Turbidity.

4. CONCLUSION

Silica inhibitors were tested at temperatures of 40 (SSI = 3.6) and 60 ˚C (SSI = 2.6) in the presence of aluminum. Although some inhibitors prevented polymerization, precipitation was observed and quantified using turbidity measurements. These inhibitors did not fully prevent the polymerization of silica and caused the precipitation and flocculation of colloids that formed. The inhibitors may disrupt the electrostatic or steric repulsion of the silica colloids, thus causing coagulation and flocculation. A combination of Inhibitors I7 and I11 prevented both polymerization and precipitation of silica at 60 ˚C. The exact mechanism of inhibition is unknown. Further studies are underway to determine the mechanism of both polymerization and precipitation inhibition of this combination.

5. ACKNOWLEDGEMENTS

The author thanks Aaron Lau for assistance with some of these experiments; Michael Bluemle, William Carey, Logan Muller, Peter Slijp and Andrew Dine for helpful discussions; and Solenis for supporting this work.

6. REFERENCES

Amjad, Z. and Zuhl, R.W.: Silica Control in Industrial Water Systems with a New Polymeric Dispersant. *Association of Water Technologies, Inc. Annual Convention & Exposition*, The Westin Diplomat, Hollywood, Fl (2009).

Amjad, Z. and Zuhl, R.W.: The Role of Water Chemistry on Preventing Silica Fouling in Industrial Water Systems. *Corrosion /2010 Conference and Exhibition*, Houston, TX (2010).

Amjad, Z.: Silica Scale Control by Non-Ionic Polymers: Influence of Water System Impurities. *Int. J. Corros. Scale Inhib.* **5**, (2016), 100-111.

Bergna, H.E. and Roberts, W.O.: Colloidal Silica: Fundamentals and Applications. Taylor & Francis, New York, (2006).

Chen, S.; Brown, K. and Jermy, M.: An explanation for the Unexpected Interactions of Silica Nanoparticles Using the Soft Particle Model, *Proceedings 40th New Zealand Geothermal Workshop*, Taupo, New Zealand (2018).

Demadis, K.D. and Neofotistou, E.: Synergistis Effects of Combinations of Cationic Polyaminoamide Dendrimers/Anionic Polyelectrolytes on Amorphous Silica Formation: A Bioinspired Approach. *Chem. Mater.* **19**, (2007), 581-587.

Demadis, K.D.; Pachis, K.; Ketsetzi, A. and Stathoulopoulou, A.: Bioinspired Control of Colloidal Silica *In Vitro* by Dual Polymeric Assemblies of Zwitterionic Phosphomethylated Chitosan and Polycations or Polyanions. *Adv. Coll. Interfac. Sci.* **151**, (2009), 33-48.

Gallup, D.L.: The Use of Reducing Agents for Control of Ferric Silicate Scale Deposition, *Geothermics*, **22**, (1993), 39-48.

Gallup, D.L.: Aluminum Sicitate Scale Formation and Inhibition: Scale Characterization and Laboratory Experiments, *Geothermics*, **26**, (1997), 483-499.

Gallup, D.L.: Investigations of Organic Inhibitors for Silica Scale Control from Geothermal Brines, *Geothermics,* **31**, (2002), 415-430.

Gallup, D.L. and Barcelon, E.: Investigations of Organic Inhibitors for Silica Scale Control from Geothermal Brines-II, *Geothermics,* **34**, (2005), 756-771.

Garcia, S.E. and Mejorada, A.V. Geogard S.X.: A Silica Scale Inhibitor for Geothermal Brine, *GRC Trans,* **25**, (2001), 15-21.

Gonzalez, W.J.; Kellogg, N.L.; Reyers Briseno, E.; Garibaldi, F. and Mora, O.: Evaluation of Various Organic Inhibitors in Controlling Silica Fouling at the CFE Cerro Prieto Geothermal Field. *GRC Annual Meeting*, Morelia, Mexico (2003).

Iler, R.K.: Coagulation of Colloidal Silica by Calcium Ions, Mechanism, and Effect of Particle Size, *J. Coll. Interfac. Sci.* **53**, (1975), 476-488.

Inanli, M. and Atilla, V.: Metal Silicate Formation at Tuzla Geothermal Brine Lines, *Proceedings International Workshop on Mineral Scaling*, Manilla, Philippines (2011).

Johnston, J.H.; Borrmann, T.; Schweig, M. and Cairns, M.J.: Elimination of the Problematic Deposition of Silica from Separated Geothermal Brine, *Proceedings 40th New Zealand Geothermal Workshop*, Taupo, New Zealand (2018).

Mavredaki, E.; Neofotistou, E. and Demadis, K.D.: Inhibition and Dissolution as Dual Mitigation Approaches for Colloidal Silica Fouling and Deposition in Process Water Systems: Functional Synergies, *Ind. Eng. Chem. Res.,* **44**, (2005), 7019-7026.

Newton, C.J.; Zarrouk, S.J.; Lawless, J.; Rowe, M.C.; Guidos, J.A. and Brown, K.L.: Aluminium-Rich Silica Scaling: San Jacinto-Tizate Geothermal Energy Project, Nicaragua, *Proceedings 40th New Zealand Geothermal Workshop*, Taupo, New Zealand (2018).

Ngothai, Y.; Lane, D.; Kuncoro, G.; Yanagisawa, N.; Rose, P. and Pring, A.: Effect of Geothermal Brine Properties on Silica Scaling in Enhanced Geothermal Systems, *GRC Trans*, **36**, (2012), 871-880.

Nishida, I.; Shimada, Y.; Saito, T.; Okaue, Y. and Yokoyama, T.: Effect of Aluminum on the Deposition of Silica Scales in Cooling Water Systems, *J. Coll. Interfac. Sci.* **335**, (2009), 18-23.

Weres, O.; Yee, A. and Tsao, L.: Kinetics of Silica Polymerization, *J Coll. Interfac. Sci.,* **84**, (1981), 379-402.

Zhang, B.; Chen, Y. and Li, F.: Inhibitory Effects of Poly(adipicacid/amine-Terminated Polyether D230/Diethylenetriamine) on Colloidal Silica Formation. *Coll. Surf. A: Phisiochem. Eng. Aspects*, **385**, (2011), 11-19.

Zhang, B.; Sun, P; Chen, F. and Li, F.: Synergistic Inhibition Effect of Polyaminoamide Dendrimers and Polyepoxysuccinic Acid on Silica Polymerization, *Coll. Surf. A: Physicochem. Eng. Aspects*, **410**, (2012), 159-169

Zhang, B.; Xin, S.; Chen, Y. and Li, F.: Synergistic Effect of Polycation and Polyanion on Silica Polymerization, *J. Coll. Interfac. Sci.,* **368**, (2012), 181-190.

Zuhl, R.W. and Amjad, Z.: In *Mineral Scales in Biological and Industrial Systems*. Amjad, Z. Ed.; CRC Press, Boca Raton, FL, (2014), p. 173-199.

7. APPENDIX

Table 4. Composition of Inhibitors.

Inhibitor	Composition
I1	Carboxylate/sulfonate copolymer
I2	Phosphonate
I3	Carboxylate/sulfonate copolymer
I4	Carboxylate/sulfonate copolymer + phosphonate
I5	Carboxylate polymer
I6	Carboxylate/ether copolymer
I7	Nonionic polymer
I8	Amine polymer
I9	Carboxylate/sulfonate copolymer
I10	Carboxylate polymer
I11	Carboxylate small molecule
I12	Carboxylate small molecule
I13	Carboxylate polymer
I14	Carboxylate polymer
I15	Carboxylate polymer
I16	Carboxylate polymer
I17	Hydroxylamine
I18	Phosphonate
I19	Carboxylate small molecule
I20	Carboxylate small molecule